Title

Deconstructing Allograft Adipose and Fascia Matrix: Fascia Matrix Improves Angiogenesis, Volume Retention, and Adipogenesis in a Rodent Model

Authors

Ziegler, Mary E
Sorensen, Alexandria M
Banyard, Derek A
et al.

Deconstructing Allograft Adipose and Fascia Matrix: Fascia Matrix Improves Angiogenesis, Volume Retention, and Adipogenesis in a Rodent Model

Mary E. Ziegler, PhD[1]
Alexandria M. Sorensen, BS[1]
Derek A. Banyard, MD, MBA, MS[1]
Lohrasb R. Sayadi, MD[1]
Evangelia Chnari, PhD[2]
Michaela M. Hatch, BS[3]
Jade Tassey, BS[1]
Yeva Mirzakhanyan, MS[3]
Paul D. Gershon, PhD[3]
Christopher C. W. Hughes, PhD[3,4,5]
Gregory R. D. Evans, MD[1]
Alan D. Widgerow, MBBCh, MMed[1]

Orange, CA; and Edison, NJ

Background: Autologous fat grafting is commonly used for soft-tissue repair (approximately 90,000 cases per year in the United States), but outcomes are limited by volume loss (20% to 80%) over time. Human allograft adipose matrix (AAM) stimulates de novo adipogenesis in vivo, but retention requires optimization. The extracellular matrix derived from superficial fascia, interstitial within the adipose layer, is typically removed during AAM processing. Thus, fascia, which contains numerous important proteins, might cooperate with AAM to stimulate de novo adipogenesis, improving long-term retention compared to AAM alone.
Methods: Human AAM and fascia matrix proteins (back and upper leg regions) were identified by mass spectrometry and annotated by gene ontology. A three-dimensional in vitro angiogenesis assay was performed. Finally, AAM and/or fascia (1 mL) was implanted into 6- to 8-week-old male Fischer rats. After 8 weeks, the authors assessed graft retention by gas pycnometry and angiogenesis (CD31) and adipocyte counts (hematoxylin and eosin) histologically.
Results: Gene ontology annotation revealed an angiogenic enrichment pattern unique to the fascia, including lactadherin, collagen alpha-3(V) chain, and tenascin-C. In vitro, AAM stimulated 1.0 ± 0.17 angiogenic sprouts per bead. The addition of fascia matrix increased sprouting by 88% (2.0 ± 0.12; $P < 0.001$). A similar angiogenic response (CD31) was observed in vivo. Graft retention volume was 25% (0.25 ± 0.13) for AAM, significantly increasing to 60% (0.60 ± 0.14) for AAM/fascia ($P < 0.05$). De novo adipogenesis was 12% (12.4 ± 7.4) for AAM, significantly increasing to 51% (51.2 ± 8.0) for AAM/fascia ($P < 0.001$) by means of adipocyte quantification.
Conclusions: Combining fascia matrix with AAM improves angiogenesis and adipogenesis compared to AAM alone in rats. These preliminary in vitro and pilot animal studies should be further validated before definitive clinical adoption. (*Plast. Reconstr. Surg.* 151: 108, 2023.)
Clinical Relevance Statement: When producing an off-the-shelf adipose inducing product by adding a connective tissue fascial component (that is normally discarded) to the mix of adipose matrix, vasculogenesis is increased and, thus, adipogenesis and graft survival is improved. This is a significant advance in this line of product.

S oft-tissue defects are often treated using autologous grafting and commercially available fillers. Approximately 90,000 patients are treated each year in the United States.[1] However, these treatments are limited by volume loss over time, showing variable resorption rates of 20% to 80% after 1 year.[2] Thus, there is a need

Disclosure: *Dr. Widgerow is chief scientific officer of Galderma and receives royalties on technology from Skin Medica; he has no conflict of interest in this study. Dr. Banyard is a paid consultant for Recros Medica, Inc.; he has no conflict of interest in this study. Dr. Chnari is an employee of MTF Biologics and participated in the study design, protocol development, manuscript review, and write-up of the allograft adipose matrix preparation methods. She did not impact the analysis or interpretation of the study results. The remaining authors have no financial interest to declare in relation to the content of this study.*

Related digital media are available in the full-text version of the article on www.PRSJournal.com.

to develop novel treatment modalities to improve graft retention.[3]

Recently, studies have explored techniques related to human adipose tissue regeneration.[4] The goal of tissue engineering (a phrase that is interchangeably used with regenerative medicine) is to regenerate damaged tissues by developing biological substitutes that maintain, restore, or improve tissue function.[5–7] One viable option for soft-tissue regeneration is human allograft adipose matrix (AAM), which is a bioscaffold for tissue regeneration.[8–14] AAM is the extracellular matrix component of allograft adipose tissue after removing the lipid and cellular components. Properly processed AAM preserves endogenous components, including matrix proteins, growth factors, and cytokines.[8,12] AAM was developed as an off-the-shelf alternative to autologous fat grafting and synthetic fillers.[15]

In preclinical models, implanting AAM in humans or mice induces adipose tissue remodeling. For instance, placing AAM in the dorsal wrist stimulates de novo adipogenesis 16 weeks after implantation, and the retention rate is 47% of the initial volume implanted.[16] In addition, in a multicenter, open-label pilot study, AAM was used to correct temple atrophy. The temple volume retention (or fullness) was established using a maximum atrophy score of 4 and a time zero score of 0 for the baseline. Volume retention over 8 weeks was highly variable (scores from 1 to 3), which decreased over the remaining weeks (scores from 0.8 to 2).[15] Thus, improving the retention of the resulting tissue after implanting AAM requires further investigation.

One avenue to improve graft survival is to ensure sufficient neovascularization.[17] A prospective study that examined fasciitis patients revealed that the fascia component of the lesion was associated with angiogenesis and vascular endothelial growth factor–producing cells to a greater degree than the muscle, as determined by immunohistochemistry.[18] When AAM is prepared, the fascia component, the continuous framework of loose connective tissue that extends throughout the body, is typically removed.[19] The fascia of interest, concerning adipose tissue, is the superficial fascia, which is derived from mesoderm and located directly under the skin and superficial adipose layers. It shows stratification grossly and microscopically and is made of membranous layers with loosely packed interwoven collagen and elastic fibers.[20]

Although fascia is traditionally regarded for its structural features, the isolation and characterization of superficial fascia–derived stromal cells from rats using flow cytometry followed by adipogenic differentiation revealed that these cells are lineage-committed preadipocytes capable of spontaneous and induced adipogenic differentiation. Thus, a new proposed model for adipogenesis involves fascial preadipocytes, which form primitive adipose lobules in subcutaneous superficial fascia.[21] Thus, given the potential association of the fascia with both angiogenesis and adipogenesis, we hypothesize that AAM, without the fascia, may be missing key functional proteins. As such, in this study, we combined fascia matrix and AAM to induce de novo adipose tissue regeneration and angiogenesis, intending to increase graft retention volume in rats.

MATERIALS AND METHODS

Cell Culture Conditions

Primary human umbilical vein endothelial cells (HUVEC) were isolated from umbilical cords obtained from local hospitals under the University of California, Irvine, Institutional Review Board approval and were cultured as described.[22] HUVEC were transduced with lentivirus-expressing green fluorescent protein and LeGO-V2 (plasmid no. 27340), from Boris Fehse (Addgene). Normal human lung fibroblasts (Lonza) were cultured in Dulbecco's Modified Eagle Medium containing 10% fetal bovine serum and 1% penicillin/streptomycin.

AAM and Fascia Preparation

The overall experimental design of this study is shown. [**See Figure, Supplemental Digital Content 1**, which shows the experimental design. Cadaveric adipose tissue was centrifuged to separate the adipose and fascia fractions. Each fraction was decellularized and powderized, creating AAM and fascia matrix. The AAM and fascia matrix were subjected to three different assays. First, they were digested and analyzed by mass spectrometry followed by gene ontology annotation. Second, the AAM and fascia matrix were used in a three-dimensional in vitro angiogenesis assay to assess the angiogenic capacity of each matrix in vitro. Lastly, the AAM and fascia matrix were implanted into rats either alone or in combination. After the tissue was harvested (at 8 weeks), it was assessed for volume retention, angiogenesis, and de novo adipogenesis, *http://links.lww.com/PRS/F518*.] The AAM and fascia matrix were obtained from human adipose

tissue recovered from cadaveric donors and were provided by MTF Biologics (Edison, NJ). Under approved protocols, the tissue was obtained following existing regulations and was screened for pathogens by serologic testing and incoming bioburden identification. The anatomical location of the recovered skin was the back and upper leg regions. The adipose tissue was recovered from the subcutaneous layer of the full-thickness skin and was separated using a semiautonomous dermatome machine and was mechanically reduced and centrifuged to isolate the adipose fraction and fascia fraction. During the initial mechanical reduction, the tissue was sheared through a stainless-steel plate containing multiple through-holes (small-diameter boreholes). The shearing action facilitated lipid removal during subsequent processing steps.

The resultant slurry of adipose and superficial fascia components was then centrifuged to separate the tissue into four layers gravimetrically (least dense to most dense), namely, the lipid (45%), adipose (40%), blood/water (5%), and fascia (10%). [**See Figure, Supplemental Digital Content 2**, which shows the separation and centrifugation of the matrices. (*Above, left*) Superficial adipose, superficial fascia, and deep adipose layers (before mechanical reduction). (*Above, right*) Example of the deep fascia/connective tissue layer observation (manually removed and discarded). (*Below*) Fractions after mechanical reduction and centrifugation, *http://links.lww.com/PRS/F519*.] Then, the adipose and fascia layers were segregated for further downstream processing. The fascia component was derived from the superficial fascia that is interstitial within the adipose tissue layer. Any residual deep fascia was removed during the initial inspection of the tissue in the upstream processing procedure.

The AAM and fascia matrix were processed in an aseptic environment in International Organization for Standardization 5 and 4 cleanrooms. The lipid component was removed using an organic solvent. A surfactant/ethanol-based solution removed the cellular content (the tissue-resident cells) and cellular debris (i.e., the organic waste left over after a cell dies) while preserving the extracellular matrix components. The matrices were decontaminated and lyophilized. Tissue sterility was verified using the United States Pharmacopeia <71> Sterility Test guidelines (Nelson Laboratories). This tissue is "shelf-ready," and further information regarding the processing of the materials is proprietary. A version of the AAM like the one used in this study is currently commercially available (RENUVA; MTF Biologics) and used in clinical studies.[16,23]

Nanoscale Liquid Chromatography Coupled to Tandem Mass Spectrometry

The AAM and fascia matrix samples were denatured in formic acid. One crystal (approximately 20 to 100 molar excess) of cyanogen bromide was added to each sample. It was digested and evaporated to dryness under vacuum, redissolved, and reduced. The samples were then ultrasonicated and diluted. Trypsin was added to an estimated enzyme-to-substrate ratio of 1:100. After an overnight digestion, a fresh equivalent of trypsin was added, and digestion proceeded for 4 hours. Then, the samples were supplemented with formic acid and desalted as described[24] using C18-SCX filters. The stacked filters were activated and washed. The C18 filters were loaded with peptides and were washed and transluted to the SCX filter. Peptides were eluted from the SCX filter. The elutions were vacuum dried and redissolved in 0.1% formic acid in water for mass spectrometry on an LTQ Orbitrap Velos Pro with EASY-nLC 1000 (ThermoFisher Scientific). Fractionation occurred on a 25×0.075 mm C18 column/electrospray tip, eluting with a linear gradient of acetonitrile in 0.1% formic acid. Precursor spectral resolution was 60,000. Peptides were identified using Mascot Server 2.6, searching against SwissProt/human and a common contaminant database allowing variable modifications of deamidation (N/Q) and oxidation (M). Precursor and fragment tolerances were 20 ppm/20 mmu, respectively; enzyme specificity was *cyanogen bromide* plus trypsin and maximum missed cleavages = 1. Bioinformatics was performed using a gene ontology analysis[25] and https://string-db.org/.

Immunofluorescence for Validation

To validate the proteins identified by mass spectrometry, the AAM and fascia matrix were pepsin digested and dried on a glass slide. Then, the samples were fixed in 4% paraformaldehyde (ThermoFisher Scientific), washed, and blocked with 5% bovine serum albumin (Sigma-Aldrich) in phosphate-buffered solution. Then, primary antibodies [anti-tenascin C (R&D Systems), anti-NG2 (Abcam), or anti-collagen VI a3 (OriGene)] in 5% bovine serum albumin were added. After washing, the samples were incubated with an Alexa Fluor 488–conjugated secondary antibody (ThermoFisher). Then, the samples were washed and imaged using an EVOS cell imaging system (ThermoFisher) (10× objective). Three fields of

view were captured for each sample, and the fluorescence intensity was quantified using ImageJ (National Institutes of Health).

Three-Dimensional Angiogenesis Assay

The three-dimensional in vitro angiogenesis assay was performed as described, with some modifications.[22] Briefly, green fluorescent protein–transduced HUVEC were coated onto Cytodex 3 microcarrier beads (Amersham Biosciences) and were embedded into a fibrin gel (MP Biomedicals). Vasculife (Life Line Cell Technology) containing normal human lung fibroblasts was added to each well, and the cultures were maintained for 10 days. This condition served as the control. The assay was carried out as described above to test the AAM and fascia matrix, but instead of fibrin alone, the AAM and fascia matrix were mixed at 75/25 (matrix/fibrin) by volume. When AAM or fascia was used at 100%, it did not gel, which is necessary for the three-dimensional in vitro angiogenesis assay. Based on previous experience with extracellular matrices derived from other tissues, adding 25% fibrin was ideal for assessing the matrix.[26] For the condition with both AAM and fascia, the 75/25 mixes were combined to make a 50/50 mix by volume of the AAM and fascia matrix. For quantification, 30 beads were randomly selected in each condition and were counted for each experiment ($n = 3$ using three different donors and for each donor there were six replicates). A sprout was only counted if it was at least as long as the diameter of the bead.

In Vivo Model

AAM and fascia matrix were reconstituted in sterile saline and subcutaneously injected in the dorsal flanks of 6- to 8-week-old male Fischer rats using a 16-gauge blunt-tip cannula (1 cc per site). Adherence to the regulations and standards set forth by the University of California, Irvine, and the National Institutes of Health Office of Animal Care and Use were strictly followed. Nine rats were assigned randomly to three groups: AAM alone, fascia alone, and 50/50 AAM/fascia (by volume) ($n = 3$ per group and each animal received four injections). The tissue (12 explants per condition) was harvested 8 weeks after implantation. Volume was assessed by gas pycnometry (Micromeritics). The explants were fixed in formaldehyde and embedded in paraffin. The tissue sections were subjected to hematoxylin and eosin staining to assess adipocytes. The number of adipocytes was counted in five fields per section at 4×. For each group, there were 12 sections. The sections were

processed using standard immunohistochemistry methods to assess vessel density. Briefly, after they were deparaffinized and rehydrated, the sections were blocked in hydrogen peroxide. Then, a trypsin enzymatic antigen retrieval kit (Abcam) was used. The subsequent processing was done using the Mouse and Rabbit Specific HRP/DAB (ABC) Detection IHC kit (Abcam) alone with the CD31 primary antibody (Novus Biologicals). The sections were mounted and imaged at 4×. Five fields of view per section were quantified using ImageJ software. For each group, there were 12 sections. The primary endpoint was to show a 50% higher volume retention in the AAM/fascia grafts than the AAM–alone grafts at 8 weeks. The secondary endpoints were to show 50% higher levels of adipocyte counts and vessels densities for the AAM/fascia grafts compared to the AAM–alone grafts at 8 weeks. The study required three animals for each group to achieve 80% power to test this hypothesis using a paired t test at a 5% significance level.

Statistical Analysis

The researchers were blinded to the experimental conditions before performing the quantifications. The statistical analyses were performed using Microsoft Excel (Microsoft Corp.) and GraphPad Prism 6 (GraphPad Software, Inc.). The in vitro data are presented as the mean ± standard error of the mean, and a t test was used to analyze the differences between the experimental groups. For the in vivo study, the data are presented as the mean ± standard deviation. A one-way analysis of variance with Tukey post hoc test was used to compare the groups. The data were considered statistically significant for values of $P < 0.05$.

RESULTS

AAM and Fascia Matrix Have Different Protein Profiles

After the mass spectrometry analysis of the AAM and fascia matrix from four donors (designated donors 1 through 4) (Table 1), the identified proteins were classified as matrisome related. A total of 42.6% of the AAM matrisome proteins and 42.9% of the fascia matrix matrisome proteins were shared between the four donors. [**See Figure, Supplemental Digital Content 3**, which shows the donor comparisons. AAM and fascia matrix from four donors were analyzed by mass spectrometry. Identified proteins were classified as matrisome-related based on The Matrisome Project (http://matrisomeproject.mit.edu/). Matrisome proteomic overlap between the four donors for AAM

111

Table 1. Donor Characteristics

Donor	Sex	Age (yr)	Height (in)	Weight (lb)	CoD
1	F	41	65	320	Unknown
2	F	60	66	195	Drug OD
3	F	51	66	209	Unknown
4	M	62	70	296	Cardiac arrest

F, female; M, male; CoD, cause of death; OD, overdose.

and fascia matrix is shown *above*. A total of 42.6% and 42.9% of the AAM and fascia matrix proteins, respectively, were shared between all four donors. The Venn diagram shows that a total of 115 and 98 matrisome proteins were identified as AAM and fascia matrix components, respectively, *http://links.lww.com/PRS/F520*.] A total of 115 and 98 matrisome proteins were identified in the adipose and fascia components, respectively. (**See Table, Supplemental Digital Content 4**, which shows all the matrisome proteins identified in each matrix by mass spectrometry, *http://links.lww.com/PRS/*

F521.) Eighty-six of these were common to the AAM and fascia matrix, 25% were unique to the AAM, and 12% were unique to the fascia matrix. The unique components of each matrix are presented in Table 2.

Mass Spectrometry Protein Identification Is Validated Using an Antibody-Based Method

Collagen VI alpha 3 was identified in both samples and had the highest Mascot score based on the mass spectrometry data. Thus, collagen VI alpha 3 was the positive control. To validate the unique proteins in the AAM and fascia matrix, we examined neural glial antigen 2 and tenascin-C, respectively. The intensity of neural glial antigen 2 in the AAM (7.35 ± 0.52) was significantly greater ($P < 0.05$) than in the fascia (1.57 ± 0.33). The intensity of tenascin-C in the fascia (7.10 ± 0.03) was significantly greater ($P < 0.05$) than in the AAM (1.85 ± 0.59). [**See Figure, Supplemental**

Table 2. Unique AAM and Fascia Matrix Proteins

Entry	Protein Name	Gene Name	Fraction
P07858	Cathepsin B	*CTSB*	AAM
Q9UBR2	Cathepsin Z	*CTSZ*	AAM
Q9H6Z9	Egl nine homolog 3	*EGLN3*	AAM
Q9BXX0	EMILIN-2	*EMILIN2*	AAM
P00734	Prothrombin	*F2*	AAM
P09038	Fibroblast growth factor 2	*FGF2*	AAM
Q14624	Inter-alpha-trypsin inhibitor heavy chain H4	*ITIH4*	AAM
P24043	Laminin subunit alpha-2	*LAMA2*	AAM
P49257	Protein ERGIC-53	*LMAN1*	AAM
O00339	Matrilin-2	*MATN2*	AAM
Q9H8L6	Multimerin-2	*MMRN2*	AAM
P31949	Protein S100-A11	*S100A11*	AAM
P06703	Protein S100-A6	*S100A6*	AAM
P05109	Protein S100-A8	*S100A8*	AAM
P06702	Protein S100-A9	*S100A9*	AAM
P08185	Corticosteroid-binding globulin	*SERPINA6*	AAM
P30740	Leukocyte elastase inhibitor	*SERPINB1*	AAM
P01008	Antithrombin-III	*SERPINC1*	AAM
P09486	Secreted protein acidic and rich in cysteine	*SPARC*	AAM
Q6PCB0	von Willebrand factor A domain-containing protein 1	*VWA1*	AAM
P01019	Angiotensinogen	*AGT*	AAM
P49747	Cartilage oligomeric matrix protein	*COMP*	AAM
P01034	Cystatin-C	*CST3*	AAM
Q6UVK1	Chondroitin sulfate proteoglycan 4	*CSPG4*	AAM
P12429	Annexin A3	*ANXA3*	AAM
Q8IUX7	Adipocyte enhancer-binding protein 1	*AEBP1*	AAM
P02746	Complement C1q subcomponent subunit B	*C1QB*	AAM
Q96CG8	Collagen triple helix repeat-containing protein 1	*CTHRC1*	AAM
Q86Y22	Collagen alpha-1(XXIII) chain	*COL23A1*	AAM
O96014	Protein Wnt-11	*WNT11*	Fascia
P24821	Tenascin-C	*TNC*	Fascia
P20908	Collagen alpha-1(V) chain	*COL5A1*	Fascia
P21980	Protein-glutamine gamma-glutamyltransferase 2	*TGM2*	Fascia
P05546	Heparin cofactor 2	*SERPIND1*	Fascia
P27658	Collagen alpha-1(VIII) chain	*COL8A1*	Fascia
Q08431	Lactadherin	*MFGE8*	Fascia
O75888	Tumor necrosis factor ligand superfamily member 13	*TNFSF13*	Fascia
P05997	Collagen alpha-2(V) chain	*COL5A2*	Fascia
Q15113	Procollagen C-endopeptidase enhancer 1	*PCOLCE*	Fascia
P25940	Collagen alpha-3(V) chain	*COL5A3*	Fascia
Q2M2W7	UPF0450 protein C17orf58	*C17orf58*	Fascia

Digital Content 5, showing validation of the mass spectrometry (*MS*) data. The AAM and fascia matrix were digested with pepsin and were coated onto glass slides. The proteins were fixed, blocked, and stained with antibodies to detect collagen VI alpha 3, neural glial antigen 2, and tenascin-C. The images were acquired using an EVOS fluorescent microscope and are presented in gray scale (*left*). *Scale bar* = 1000 μm. (*Right*) Quantified data, which are the average of two of the donor samples, with three fields of view from each donor, and are expressed as the fluorescence intensity in arbitrary units (*AU*), as measured using ImageJ software. The data are presented as the mean ± SEM (*n* = 3; five fields were counted per condition; *P < 0.05), *http://links.lww.com/PRS/F522*.]

Functional Annotation Reveals a Unique Angiogenic Profile for the Fascia Matrix

The gene ontology analysis demonstrated that for biological process, 224 pathways were common to the two samples. However, examining the top 40 enriched biological process pathways in each sample revealed unique pathway enrichments (Table 3). Pathways related to angiogenesis were identified in the fascia matrix. These were not enriched in this portion of the pathways from the AAM sample. Next, six pathways were unique in the AAM for molecular function, and there were three unique pathways in the fascia matrix (Table 3). These findings indicated that the AAM showed an enriched binding capacity compared to the fascia matrix. Finally, for the cellular component category, five pathways were unique for the AAM, and three were unique for the fascia matrix (Table 3). These unique cellular component pathways indicated that the AAM was associated with proteins related to cell parts, whereas the fascia was enriched for components related to collagen.

Fascia Matrix Supports Angiogenic Sprouting

The average number of angiogenic sprouts per bead for the AAM condition was 1.0 ± 0.12. The fascia matrix produced 4.1 ± 0.21 sprouts per bead, which was a significant increase (294%) (P < 0.001). Not surprisingly, the control wells, with pure fibrin, gave the most robust response (6.9 ± 0.17 sprouts per bead). When the AAM and fascia matrix were mixed (50/50 by volume), this combination showed an average of 2.0 ± 0.17 sprouts per bead. The difference between the AAM and the mixed condition was significant (88% increase; P < 0.001). [**See Figure, Supplemental Digital Content 6**, which shows the in vitro angiogenesis data. (*Left*) Green fluorescent protein–transduced HUVEC were coated onto Cytodex beds and embedded in variety of extracellular matrix gels. Control assay: HUVEC–coated beads were embedded in a fibrin gel. AAM assay: HUVEC–coated beads were embedded in a gel made of 75% AAM and 25% fibrin. Fascia matrix assay: HUVEC–coated beads were embedded in a gel made of 75% fascia matrix and 25% fibrin. AAM/fascia mix assay: HUVEC–coated beads were embedded in a gel made of 75% AAM and fascia (a 50:50 mix) and

Table 3. Unique Pathway Enrichments

	AAM	Fascia
Biological process	Regulation of endopeptidase activity	Regulation of cell-substrate adhesion
	Negative regulation of proteolysis	Positive regulation of cell-substrate adhesion
	Regulation of wound healing	Single-organism catabolic process
	Negative regulation of cellular process	Blood vessel development
	Single-multicellular organism process	Vasculature development
	Negative regulation of wound healing	Cell-substrate adhesion
	Negative regulation of biological process	Regulation of cell adhesion
	Glycosaminoglycan catabolic process	Vesicle-mediated transport
	System development	Peptide cross-linking
	Multicellular organismal process	Cell-matrix adhesion
	Cell activation	Blood vessel morphogenesis
	Negative regulation of protein metabolic process	
Molecular function	S100 protein binding	Molecular function regulator
	RAGE receptor binding	Carbohydrate derivative binding
	Toll-like receptor 4 binding	Peptidase activator activity
	Identical protein binding	
	Cysteine-type endopeptidase inhibitor activity	
	Arachidonic acid binding	
Cellular component	Organelle	Collagen type V trimer
	Cytoplasmic vesicle part	Network-forming collagen trimer
	Golgi apparatus part	Macromolecular complex
	Side of membrane	
	Perinuclear region of cytoplasm	

25% fibrin. The gels were fixed and imaged at 10 days. *Scale bar* = 400 μm. The sprouts were counted from 30 beads per condition, and the average and standard error of the mean are presented (*n* = 3 using three different donors and for each donor there were six replicates; ***P* < 0.001). (*Right*) Fischer rats were implanted subcutaneously with AAM, fascia matrix or a mix of 50/50 AAM and fascia matrix into the dorsum (four implants per animal; *n* = 3 animals per group). After 8 weeks, the explants (12 per group) were embedded in paraffin and sectioned, and the endothelial cells within the sections were visualized by staining for CD31+ cells. The arrows indicate the positive vessel staining. *Scale bar* = 100 μm. Vascular density was calculated using ImageJ. Five representative areas from each section were used for the calculations (**P* < 0.05), *http://links.lww.com/PRS/F523*.]

Adding Fascia Matrix to AAM improves Angiogenesis, Volume Retention, and Adipogenesis In Vivo

Eight weeks after implantation, the tissue harvested from the rats revealed that there was a statistically significant increase in CD31⁺ cells when the fascia matrix alone (214.2 ± 4.0) was implanted compared to the AAM alone (175.1 ± 4.0; 23% increase; *P* < 0.05). The increase for the 50/50 mixture (183.7 ± 3.3; 7% increase; *P* < 0.05) was also statistically significant compared to the AAM alone. The difference between the fascia alone and the 50/50 group was not significant (*P* > 0.05) (**see Figure, Supplemental Digital Content 6**, *http://links.lww.com/PRS/F523*).

Furthermore, implanting fascia alone and the 50/50 mixture resulted in significantly greater volume retentions (0.70 ± 0.08 and 0.60 ± 0.14, respectively; *P* < 0.05 for both) compared to the AAM alone (0.25 ± 0.13). The difference between the fascia alone and the 50/50 group was not significant (*P* > 0.05). [**See Figure, Supplemental Digital Content 7**, which shows volume retention. The explants were imaged to demonstrate the size differences visually. *Scale bar* = 5 mm. A volume assessment was performed on all the explants using a gas pycnometer. The data are presented as the mean ± SEM (*n* = 12 per condition; **P* < 0.05), *http://links.lww.com/PRS/F524*.]

Finally, we examined de novo adipogenesis. The percentage adipose area of the 50/50 group was statistically significantly greater than the AAM–alone group (51.2 ± 8.0 and 12.4 ± 7.4; *P* < 0.001). The difference between the AAM (12.4 ± 7.4) and fascia groups (23.5 ± 7.9) was not significant (*P* > 0.05) (Fig. 1).

DISCUSSION

Determining the matrisome constituents of AAM and fascia matrix is essential for understanding function. The mass spectrometry analysis and annotation of these extracellular matrix proteins revealed that the fascia matrix showed a greater enrichment for angiogenesis-related pathways than the AAM, leading to the hypothesis that the fascia matrix might contain factors that contribute to angiogenesis during adipoinduction.

Previously, an array of angiogenic-related extracellular matrix proteins was identified using a three-dimensional in vitro angiogenesis assay.[27] Among these proteins, ANXA2, COL1A1, FN, COL1A2, TGFB1, and LAMC1 were present in the AAM and fascia matrisomes from all four donors. In addition, SPARC was identified in three donors in the AAM, and PCOLCE was identified in two donors in the fascia matrix. The AAM and fascia matrix were used in the same three-dimensional in vitro angiogenesis assay. AAM poorly supported angiogenesis. However, the fascia induced robust sprouting (an increase of 294% compared to AAM), and adding fascia to the AAM stimulated sprouting angiogenesis (an increase of 88%). These findings supported the bioinformatics data, revealing that fascia matrix was angiogenic. Part of the mechanism by which extracellular matrix proteins regulate angiogenesis is by increasing the stiffness of the extracellular matrix.[27] The AAM and fascia matrix are composed of different extracellular matrix proteins related to angiogenesis. Thus, understanding the balance of the AAM and facia matrix proteins will be important for assessing the stiffness of the matrices in the three-dimensional angiogenesis assay.

Implanting the fascia alone and the 50/50 mix of AAM and fascia in rats showed an enhanced vessel density at 8 weeks compared to AAM alone (23% and 7% increases, respectively), suggesting that adding fascia matrix enhanced the angiogenic capacity of AAM. Previously, when AAM alone was implanted in mice, it stimulated angiogenesis to a greater degree (>50% increase in vessel density) compared to fat grafting.[28] Thus, adding fascia to AAM should improve angiogenesis in the graft compared to fat grafting.

Here, AAM supported adipogenesis, which was significantly improved at 8 weeks by adding fascia, increasing from 12% to 51%. However, fascia alone did not significantly improve adipogenesis (23%) compared to AAM. In addition, the volume retention after 8 weeks for the AAM group was only 12.4% but increased to 60% in the AAM/fascia group. The fascia alone
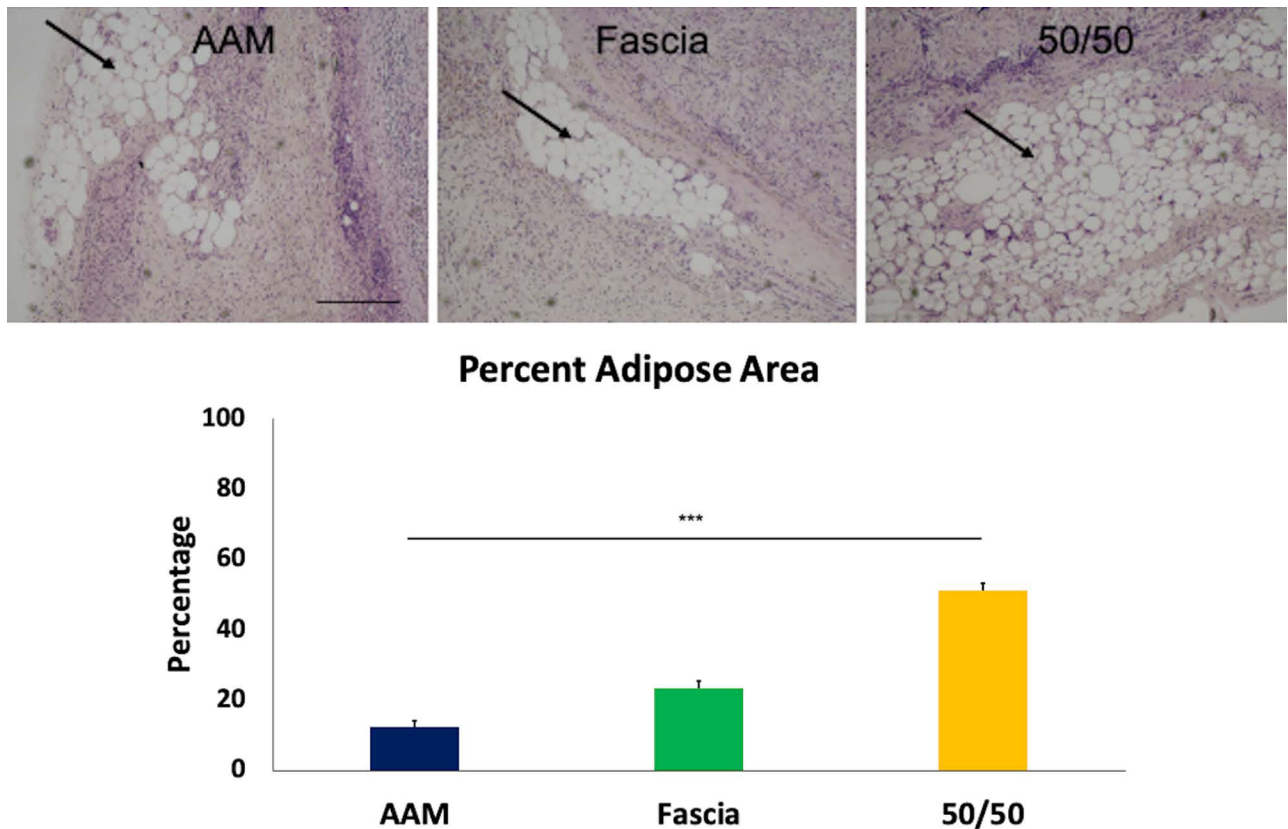
114

Fig. 1. De novo adipogenesis. (*Above*) After 8 weeks, the explants (12 per group) were paraffin embedded, sectioned, and hematoxylin and eosin stained. Adipocytes within the sections were visualized by microscopy. The *arrows* indicate areas of adipocytes. *Scale bar* = 100 μm. (*Below*) De novo adipogenesis was assessed by counting the number of adipocytes in each explant relative to the entire area of the section. Five representative areas from each section were used for the calculations. The data are presented as the mean ± SEM (*n* = 12 per condition; ***$P < 0.001$).

group revealed the largest volume retention at 70%. Together with the adipogenesis data, these findings reveal that the best scaffold for supporting volume retention, along with adipogenesis, was demonstrated when AAM included the fascia component. Previously, when AAM was implanted in mice, volume retention was improved by 61% compared to fat grafting. This was further improved to 82% when the AAM was combined with external volume expansion.[28] Thus, AAM performs better than fat grafting with respect to volume retention. Our data suggest that when fascia is added, this improvement could be even more significant (Fig. 2).

Given that the AAM used here is similar to Renuva Allograft Adipose Matrix, we propose that the indications/contraindications would be similar. This AAM/fascia matrix would be intended for the replacement of damaged or insufficient integumental adipose tissue matrix in areas where native fat already exists. In addition, it might also be used as reinforcement or supplemental support for underlying adipose tissue matrix as the result of damage or naturally occurring defects. The contraindications would be that it should not be injected in an area where native adipose does not typically exist and that it should not be used for patients with severe allergy sensitivities.

This study has several limitations that deserve attention with respect to future experiments. First, the mass spectrometry–based proteomic methods used were qualitative rather than quantitative. To provide further information on the composition of these matrices, in the future, we might use label-free mass spectrometry methods to quantify the individual peptide concentrations.[29] Second, the in vivo study only examined one time point. Ongoing studies in our laboratory examine the grafts over time, for a longer period and with more animals per condition. This is a crucial goal for better understanding the translatability of these studies. Third, these results should be compared to lipoaspirate or cell-assisted lipotransfer in an animal model. However, because most of the animal models
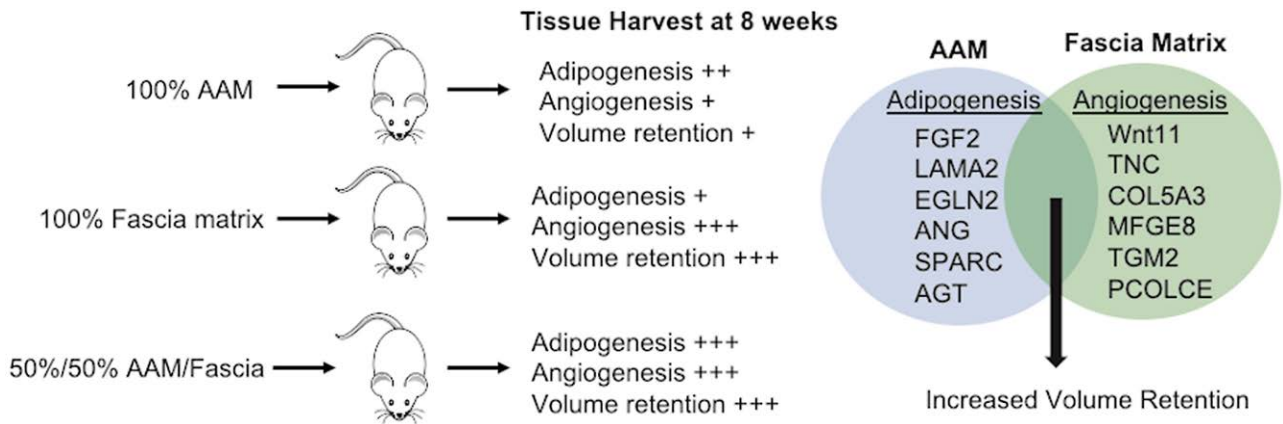
Fig. 2. Proposed mechanism. When 100% AAM is implanted in rats, after 8 weeks, it moderately activates (as indicated by the ++) de novo adipogenesis, in relation to the volume of the tissue. Angiogenesis is also activated at a low level (+), but volume retention is poor (+). When 100% fascia matrix is implanted in rats, after 8 weeks, there is a low level of de novo adipogenesis (+) in relation to the volume of the tissue. Angiogenesis is strongly activated (+++) and volume retention is high (+++). When the AAM and fascia matrix were implanted together (50/50), all of the measured outcomes show significantly improved responses compared to AAM alone. Together, these data show that AAM is valuable for generating de novo adipose tissue (unique proteins identified by mass spectrometry are shown), fascia matrix is a potent angiogenesis stimulator (unique proteins identified by mass spectrometry are shown) and generates volume, but the tissue is not largely adipose in nature. However, the combination of AAM and fascia matrix generates de novo adipose tissue that is vascularized with a large volume retention.

in the literature use mice or athymic rats and we used immunocompetent rats, in the future, we plan to incorporate these comparisons using the appropriate model. Finally, further studies exploring the elasticity, stiffness, and compressive properties of these matrices alone and in combination with respect to the matrisome proteins identified would extend the scope of the current data.

CONCLUSIONS

In summary, we deconstructed the components of AAM and fascia matrix and determined that the angiogenic properties of these matrices were differential. Given the close relationship between angiogenesis and adipogenesis, we also revealed that retaining the fascia matrix within the AAM created an improved bioscaffold that can potentially be used off-the-shelf for tissue regeneration. If these initial preliminary findings are confirmed and validated, the fascia matrix and AAM combination could be used for soft-tissue reconstruction in various clinical conditions.

Alan D. Widgerow, MBBCh, MMed
Center for Tissue Engineering
Department of Plastic Surgery
University of California, Irvine
101 South City Drive, Suite 108a, Building 55
Orange, CA 92868
awidgero@uci.edu
@alanwidge

REFERENCES

1. Cosmetic surgery national data bank statistics. *Aesthet Surg J.* 2018;38:1–24.
2. Gause TM II, Kling RE, Sivak WN, Marra KG, Rubin JP, Kokai LE. Particle size in fat graft retention: a review on the impact of harvesting technique in lipofilling surgical outcomes. *Adipocyte* 2014;3:273–279.
3. Patrick CW Jr. Tissue engineering strategies for adipose tissue repair. *Anat Rec.* 2001;263:361–366.
4. Mahoney CM, Imbarlina C, Yates CC, Marra KG. Current therapeutic strategies for adipose tissue defects/repair using engineered biomaterials and biomolecule formulations. *Front Pharmacol.* 2018;9:507.
5. Atala A. Tissue engineering and regenerative medicine: concepts for clinical application. *Rejuvenation Res.* 2004;7:15–31.
6. Langer R. Biomaterials in drug delivery and tissue engineering: one laboratory's experience. *Acc Chem Res.* 2000;33:94–101.
7. Langer R, Vacanti JP. Tissue engineering. *Science* 1993;260:920–926.
8. Banyard DA, Borad V, Amezcua E, Wirth GA, Evans GR, Widgerow AD. Preparation, characterization, and clinical implications of human decellularized adipose tissue

extracellular matrix (hDAM): a comprehensive review. *Aesthet Surg J.* 2016;36:349–357.

9. Choi JS, Kim BS, Kim JY, et al. Decellularized extracellular matrix derived from human adipose tissue as a potential scaffold for allograft tissue engineering. *J Biomed Mater Res A* 2011;97:292–299.

10. Flynn LE. The use of decellularized adipose tissue to provide an inductive microenvironment for the adipogenic differentiation of human adipose-derived stem cells. *Biomaterials* 2010;31:4715–4724.

11. Porzionato A, Sfriso MM, Macchi V, et al. Decellularized omentum as novel biologic scaffold for reconstructive surgery and regenerative medicine. *Eur J Histochem.* 2013;57:e4.

12. Sano H, Orbay H, Terashi H, Hyakusoku H, Ogawa R. Acellular adipose matrix as a natural scaffold for tissue engineering. *J Plast Reconstr Aesthet Surg.* 2014;67:99–106.

13. Wang L, Johnson JA, Zhang Q, Beahm EK. Combining decellularized human adipose tissue extracellular matrix and adipose-derived stem cells for adipose tissue engineering. *Acta Biomater.* 2013;9:8921–8931.

14. Young DA, Ibrahim DO, Hu D, Christman KL. Injectable hydrogel scaffold from decellularized human lipoaspirate. *Acta Biomater.* 2011;7:1040–1049.

15. Gold MH, Kinney BM, Kaminer MS, Rohrich RJ, D'Amico RA. A multi-center, open-label, pilot study of allograft adipose matrix for the correction of atrophic temples. *J Cosmet Dermatol.* 2020;19:1044–1056.

16. Kokai LE, Schilling BK, Chnari E, et al. Injectable allograft adipose matrix supports adipogenic tissue remodeling in the nude mouse and human. *Plast Reconstr Surg.* 2019;143:299e–309e.

17. Yu Q, Cai Y, Huang H, et al. Co-transplantation of nanofat enhances neovascularization and fat graft survival in nude mice. *Aesthet Surg J.* 2018;38:667–675.

18. Yoshida K, Ito H, Furuya K, Ukichi T, Noda K, Kurosaka D. Angiogenesis and VEGF-expressing cells are identified predominantly in the fascia rather than in the muscle during the early phase of dermatomyositis. *Arthritis Res Ther.* 2017;19:272.

19. Schleip R, Jäger H, Klingler W. What is 'fascia'? A review of different nomenclatures. *J Bodyw Mov Ther.* 2012;16:496–502.

20. Kumka M, Bonar J. Fascia: a morphological description and classification system based on a literature review. *J Can Chiropr Assoc.* 2012;56:179–191.

21. Su X, Lyu Y, Wang W, et al. Fascia origin of adipose cells. *Stem Cells* 2016;34:1407–1419.

22. Nakatsu MN, Davis J, Hughes CC. Optimized fibrin gel bead assay for the study of angiogenesis. *J Vis Exp.* 2007;186.

23. Shahin TB, Vaishnav KV, Watchman M, et al. Tissue augmentation with allograft adipose matrix for the diabetic foot in remission. *Plast Reconstr Surg Glob Open* 2017;5:e1555.

24. Rappsilber J, Mann M, Ishihama Y. Protocol for micropurification, enrichment, pre-fractionation and storage of peptides for proteomics using StageTips. *Nat Protoc.* 2007;2:1896–1906.

25. Glass K, Girvan M. Annotation enrichment analysis: an alternative method for evaluating the functional properties of gene sets. *Sci Rep.* 2014;4:4191.

26. Romero-López M, Trinh AL, Sobrino A, et al. Recapitulating the human tumor microenvironment: colon tumor-derived extracellular matrix promotes angiogenesis and tumor cell growth. *Biomaterials* 2017;116:118–129.

27. Newman AC, Nakatsu MN, Chou W, Gershon PD, Hughes CC. The requirement for fibroblasts in angiogenesis: fibroblast-derived matrix proteins are essential for endothelial cell lumen formation. *Mol Biol Cell* 2011;22:3791–3800.

28. Giatsidis G, Succar J, Waters TD, et al. Tissue-engineered soft-tissue reconstruction using noninvasive mechanical preconditioning and a shelf-ready allograft adipose matrix. *Plast Reconstr Surg.* 2019;144:884–895.

29. Schubert OT, Röst HL, Collins BC, Rosenberger G, Aebersold R. Quantitative proteomics: challenges and opportunities in basic and applied research. *Nat Protoc.* 2017;12:1289–1294.